EXPERIMENTAL INVESTIGATION ON THE EFFECT OF BIOMIMETIC TUBERCLES ON THE HYDRODYNAMICS OF A FLAT PLATE

Roberto Ravenna, University of Strathclyde UK/University of Trieste Italy
Alessandro Marino, University of Strathclyde, UK
Soonseok Song, University of Strathclyde, UK
Yigit Kemal Demirel, University of Strathclyde, UK
Mehmet Atlar, University of Strathclyde, UK
Osman Turan, University of Strathclyde, UK

A means of reducing the hydrodynamic resistance of ships would dramatically reduce their fuel consumption, leading to reduced carbon emissions worldwide. The ITTC recommends researchers to develop new formulae or methods, using experimental data, for the prediction of the effects of the surface on ship resistance. This research was carried out towards this perspective and presents the results obtained during the tests conducted at the towing tank facilities of the University of Strathclyde
The aim of this paper was to answer the question, "Could the biomimetic tubercles improve the hydrodynamic efficiency of a flat plate?". Conveniently prepared flat plates were towed at a range of speed up to 4.5 m·s, parallel to the water flow.
The experimental investigation on the effect of biomimetic tubercles on the performance of the flat plate is based on the use of 3-D printed pieces modelled as the tubercles which appears on the head of humpback whales. The tubercles were positioned on the plate in different configurations and it was found that, in the range of speed tested, their application in rows, upstream of the flat plate, gives the maximum drag and total resistance coefficient reductions of -1,7% and -1,3%, respectively.
Keywords: biomimetic tubercles, towing tank, flat plate, drag, resistance coefficients.

1. Introduction

In the past, technology was a means of dominating nature and inventions were products of our imaginations. Today, the relationship between engineering and biology is being reversed. In 1950s the name biomimetics was coined for the transfer of ideas and analogues from biology to technology [1]. Nature is now being considered as the template for improving mechanical devices and operations and developing whole new technologies [2], [3], [4], [5], [6], [7], [8].
The goal of this approach is to engineer systems that emulate the performance of living systems or their constructs, particularly in instances in which an organism's performance exceeds current human-engineered technologies [9], [10], [11], [12].
It is essential to consider that, although shipping is marginally more environmentally friendly than other forms of transportation, such as aviation and land, the International Maritime Organisation (IMO) reported in 2015 that ships release about 2,8% of the total CO_2 emissions a year [13].
According to RAEng (2013), 95% of the world's cargo is transported by sea. It is in public awareness that, as for other means of pollution, making the ships more energy efficient is of great importance to reduce the greenhouse gases and CO2 release in the atmosphere. Hence, new regulations are periodically issued by IMO to implement the energy efficiency of ships.
Hull resistance is of paramount importance to ships since it directly affects their speed, power requirements and fuel consumption [14]. A means of reducing the hydrodynamic resistance of the hull would extremely improve the Energy Efficiency Design Index (EEDI) of the ship by dramatically reducing their fuel consumption [15]. The total resistance of a ship is made up of a number of different components, which are caused by a variety of factor which interact one with the other in an extremely complicated way. For conventional displacement ships it is known that frictional resistance is the

largest single component of the total resistance of a ship, indeed, experiments have shown that even in smooth, new ships it accounts for 80 to 85 percent of the total resistance [16]. According to [17], skin friction can account for up to 90% of the total resistance, for a slow-speed ship.
The problem essence is from both economic and environmental points of view in terms of increased resistance, increased fuel consumption, increased greenhouse gases emissions and transportation of harmful non-indigenous species. The International Towing Tank Conference (ITTC) therefore recommends researchers to develop new methods, using experimental data, to improve the efficiency of ship resistance [18].
The International Towing Tank Conference (ITTC) therefore recommends researchers to develop new methods, using experimental data, to improve the efficiency of ship resistance [18].
Biomimetic tubercles are a representation of particular warty round outgrowths exhibited by multiple organisms such as Humpback whales (*Figure 1).* Tubercles are reported on the leading-edge of the pectoral fins and on the head of humpback whales (*Megaptera Noveangliae*) during scientific observations [19], [20]. The function of the tubercles of the head is sensorial too, [21]. Indeed, their inner structure is highly innervated, as Pacinian corpuscles in terrestrial mammals [21].
The tubercles on the pectoral fins were demonstrated to improve fluid flow over the flipper's surface, exhibiting the so-called *tubercle effect* of fluid dynamics [8], [22]. They enhance the manoeuvrability of the humpback whales which are incredibly agile, capable of quick movements and underwater acrobatics. Thus, despite their bulky bodies, these huge mammals are here as our template.

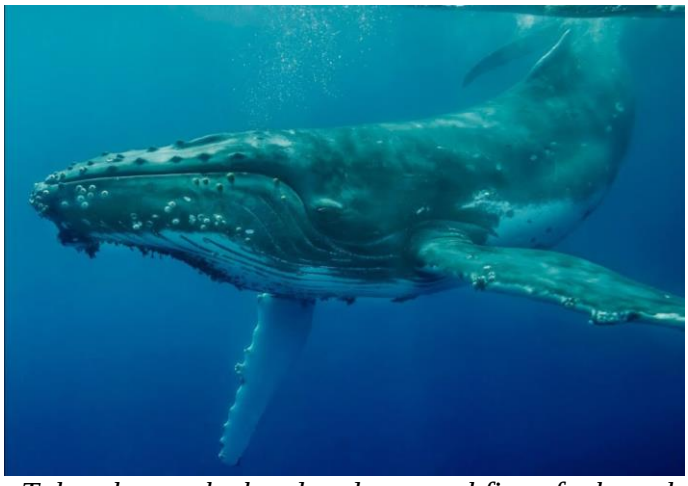

Figure 1 – Tubercles on the head and pectoral fins of a humpback whale

Extensive research has been carried out for the leading-edge biomimetic tubercles on flat plates, foils and wing profiles, [23], [24], [25], [26], [27].
The aeronautical application of leading-edge tubercles on foils and wings, discussed in [8], represents the major part e.g., wind tunnel studies of leading-edge sinusoidal tubercles on flat plates as in [28].
The positive influence of these protuberances to the overall performance has been highlighted, despite a possible slight increase in the drag of these objects, due to more extensive energy exchange with the fluid.
Although the phenomena that occurs to the flow are uncertain, all the authors agree that the possible reason can be found in the impact of the tubercles on the wake decay or lift and drag fluctuations [27].
They acknowledge that the tubercles produce streamwise contra-rotating vortices, which are believed to alter the boundary layer and the flow direction within.
Miklosovic et al. [26] propose one of the several theories summarized in [27] that attempt to describe the tubercle effect. They compare the tubercles to vortex generators, induced flow, vortex lift and compartmentalisation theories.

Remarkable is also the marine application of leading-edge tubercles on hydrofoils, extensively studied by several researchers, such as for rudders [29] or tidal turbines [30], [31].
The experiments described in [29] carried in a water channel studied the effect of sinusoidal tubercles on lift, drag and cavitation onset of rudder. The authors found that adding tubercles to the leading edge of the rudder induced an earlier occurrence of stall but, while the drag increased after stall, the lift remained almost constant, unlike the case of a regular rudder, where the lift has a drastic drop in the stall region. They also found that, comparing the tubercle rudder to a standard one, at high Reynolds numbers there was a higher drag coefficient while at low Reynolds number there was no penalty. The towing tank experiments conducted by Gruber et al. [31] on a set of tidal turbine blades proved that the leading-edge tubercles improve the overall performance of the tidal turbine.
An important finding of Shi et al. [30] in their studies on tidal turbine blades, also confirmed that cavitation occurred at lower angles of attack, but it was confined in the areas between tubercles.
The leading-edge tubercles improvement is believed to be due to the reduction of flow separation and inhibition of stall [32], as observed in numerical simulations and detected by Particle Image Velocimetry (PIV) measurements.
It was found that more energy is transmitted into the flow by the tubercles. This led to the reduction in the flow separation at the cost of a slight increase of drag. The lower velocity in the wake field, which results in higher power and thrust coefficients is due to this higher induction factor of the tubercles.
The position of the tubercles on the head of humpback whales, although scientists suggested that they could have a tactile function, may also suggest that their interaction with the fluid is optimal when the flow is laminar.
To the author's best knowledge, except the ongoing CFD research of Marino et al. [33], no other studies have been carried out on the effect of these particular tubercles on the hydrodynamics of a marine structure, either a simple submerged flat plate or a ship hull.
As discussed above, the hydrodynamic efficiency of ships is crucial for a naval architect. Therefore, this article focuses on a unique innovative possibility of improving the hydrodynamic efficiency of the hull by means of humpback whale-like tubercles.
In summary, answering the question, "Could the biomimetic tubercles improve the hull hydrodynamic efficiency?" is the aim of this research.
Specific objectives are to find, by means of Experimental Fluid Dynamics (EFD), feasible configurations of biomimetic tubercles which could improve the hydrodynamics of a flat plate.
It is known by experience [34] that on the hull of a ship, there are areas more affected by biofouling than others, due to several reasons. One of the reasons is the lack of turbulence which helps the water to stagnate and, thus, the biofouling to grow. The application of tubercles in a weak portion of the hull, despite a controllable increase of drag, would introduce the desired turbulence in the flow that helps to retard the degradation of the hull due to biofouling [35].
Above all, other objectives will be outlined along the way of this paper and the results of the study will be discussed, along with recommendations for future avenues of research. Novel contributions are ought to be made to the state-of-the-art knowledge.

2. Methodology

The towing tank tests at the Kelvin Hydrodynamics Laboratory (KHL) of the University of Strathclyde (UK) were carried following the state-of-the-art procedures suggested in [36].
Four tubercles configurations were tested, and the bare plate was towed at the same range of speed (from 1.5 to 4.5 m/s with an increment of 0.2 m/s) for reference. The uncertainty was evaluated by repeating the runs at the lowest and highest speeds at least two more times, for each configuration.
The total resistance (drag) of a flat plate (R_T), can be decomposed in just two major components: the frictional resistance (R_F) and the residuary resistance (R_R), as given in (1):

$$R_T = R_F + R_R \quad (1)$$

The frictional resistence occurs due to shear stresses on the plate's surface. The residuary resistance arises due to the wave making resistance since the pressure resistance component is neglegible for thin bodies [16].
The values of the total resistance (R_T) measured by the trasducers were non-dimensionalised to obtain the total resistance coefficient (C_T), as follows in the equation (2):

$$C_T = \frac{R_T}{\frac{1}{2}\rho S V^2} \quad (2)$$

Where: (ρ) is the water density; (S) the wetted surface or the flat plate (not including the neglegible added surface of the tubercles); (C_T) is the total resistance coefficient; (V) is the towing speed.
Similarly to (R_T), the total resistance coefficient (C_T) is made up of the frictional coefficient (C_F), function of the Froude number, (Fn), and residuary resitance coefficient (C_R) function of the Reynolds number (Rn), as in equation (3) from [16], [37]:

$$C_T = C_F(Rn) + C_R(Fn) \quad (3)$$

The differences between the (C_T) values obtained from experiments and the (C_F)values obtained using Hughes's frictional line [38], [39] (Equation (5)) were the (C_R) values for the Reference Plate, as shown in the Equation (4):

$$C_R = C_T - C_F \quad (4)$$

For a smooth plate, the frictional resistance coefficients can be predicted using the frictional correlation line of Hughes [38], [39], Equation (5):

$$C_F = \frac{0{,}066}{(log(Rn) - 2.03)^2} \quad (5)$$

Since they were not expected to be effectively affected by the tubercles [37], the values of the residual resistance coefficients (C_R) of the bare flat plate (reference) were assumed to be the same for all the other configurations (tubercled).
In the Results section, a conversion of the results to a nominal temperature of 15°C for comparison was made so that future similar studies could more readily benefit of the findings.
The preparation of the flat plate models and their towing tests were carried at KHL [40].
The KHL fresh water test tank is 76.0 metres long, 4.6 metres wide and 2.5 metres deep. It is equipped with a digitally controlled towing carriage, a state-of-the-art absorbing wave maker, and a highly effective sloping beach. The carriage (*Figure 2*) has a velocity range of 0÷5 m/s, with the velocity range used in these experiments kept between 1.5 and 4.5 m/s.
The computer based modular data acquisition/control system has up to 64 input and 20 output channels and a sampling rate up to 60kHz. The temperature of the water was monitored in order to be able to evaluate drag coefficients according to the actual temperature.

Figure 2- Towing carriage of KHL

The resistance transducers were calibrated with weights following the procedure of [41] and [42] at 95% confidence level.
Two displacement transducers were used to measure respectively the drag and the side force of the towed plate. The transducers from Cambridge Electronic Design (CED) 1988-2016 – Data Acquisition & Analysis used the Linear Variable Differential Transformer (LVDT) principle. Spike2 version 8.09b x64 Unicode was the software utilised to digitalise the signals.
The flat plate was manufactured from 304 stainless steel grade sheet stock, it had the dimensions given in the Table 1 below:

Table 1 – Dimensions of the flat plate in metres

Length	1.495
Height	0.805
Thickness	0.005
Draught	0.588

The leading (upstream) and trailing (downstream) edges of the flat plate were milled and the whole plate was polished with acetone solvent. In particular, the leading edge was rounded with a radius of 2.5 mm, while the trailing edge was kept flat sharp. The flatness of the plate was checked before starting the tests.
All these steps were done in order to reduce the undesired extra drag and lift of the bare flat plate.
Once the plate was installed on the rig of the carriage, repeated runs were conducted to find the correct alignment. The side forces were monitored during all the set of runs and, once found the optimal position, no further adjusments were made on the alignment of the plate.
The repeated tests were performed to estimate the uncertainty for the drag coefficients at the lowest and highest speeds of the range (1.5 and 4.5 m/s, respectively). For this estimate, the procedure of [41], [42] and [43] was followed, similarly as for the calibration of instruments.

3. Tests

For each configuration, the plate was towed longitudinally (*Figure 3*) at a range of speeds and the drag measured. The frictional resistance coefficients according to Hughes, equation (5) was used to calculate the frictional and then resisduary coefficients of the flat plate. Then, the actual frictional coefficients were found substracting (C_R) to the experimental (C_T).
With an increment of 0.2 m/s, the whole range of speed from was tested and two repeats at the lowest and highest speed of the range were always carried out for repeatability and uncertainty analysis.

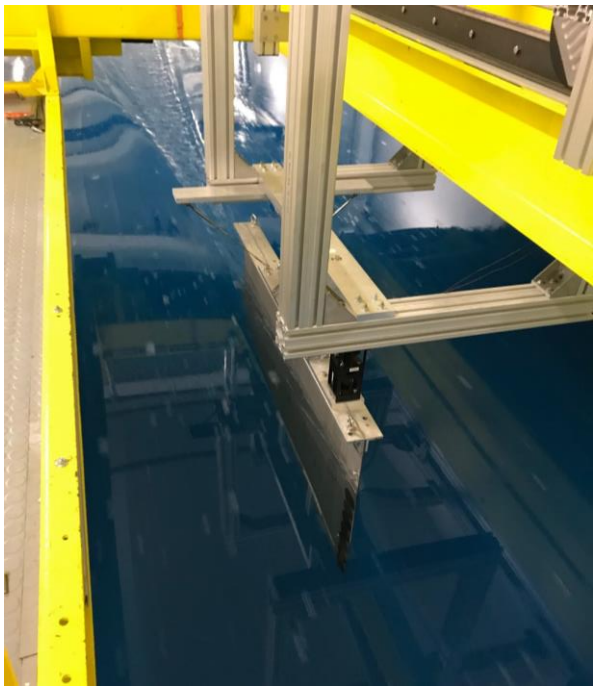

Figure 3 - Flat plate towed at 4.5 m/s

The geometry model of a biomimetic tubercle (*Figure 4*) was chosen according to Marino et al. [33]. They resembled the anatomy findings of scientists described in [21] for the tubercle of the head of humpback whales (*Table 2*).

Table 2 – Details of tubercles on the head of a calf humpback whale

Tubercle dimensions	Humpback whale calf	Biomimetic model
Height	7÷25 mm	10 mm
Basal circumference	57÷120 mm	74 mm

The sinusoidal defining the top boundaries has a wavelength of 74 mm and a height of 10 mm. The basal diameter length of 74 mm was chosen in order to cover the breadth of the plate with a suitable number of tubercles [33].
The geometrical model was implemented using Rhinoceros in order to be easily 3D printed. The model was axisymmetric and presented a basal circumference whose thickness was kept to the minimum printable of 0.1 mm. The convexity and the presence of stagnation points were checked in order to obtain a good quality of printings. The tubercles were 3-D printed using an Ultimaker printer. Each tubercle was smoothened using sand paperer of 400 grit (recommended by ITTC [18]). The method adopted to stick the tubercle shaped plates on the flat plate was covering the base with a very thin double face tape.

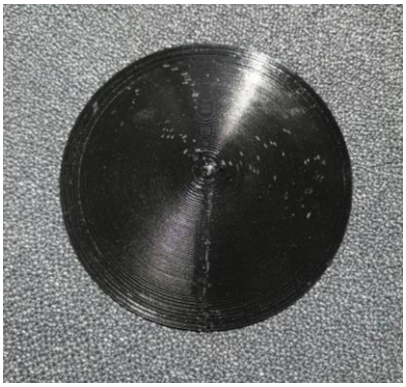

Figure 4 - 3D printed tubercle

The different configurations of tubercles to test were designed using AutoCAD. The area of the tubercles in the three row configurations was made to be axisymmetric with respect to the longitudinal barycentric axis of the wetted surface of the plate.
Similarly, the centre of area of the distributed configuration of tubercles corresponded the centre of area of the wetted surface of the plate. The symmetry with respect to the barycentric axis reduced the side forces and lift of the plate.
The configurations of tubercles adopted for the flat plate were four, as listed below and showed in (*Figure 5*): a) Distributed, b) Mid-length, c) Upstream, d) Downstream.

a) 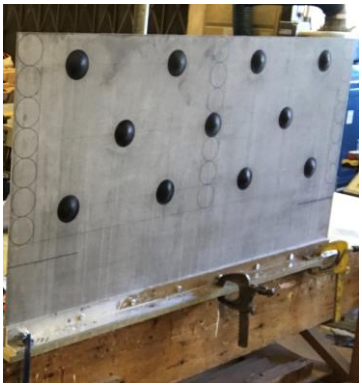 b) 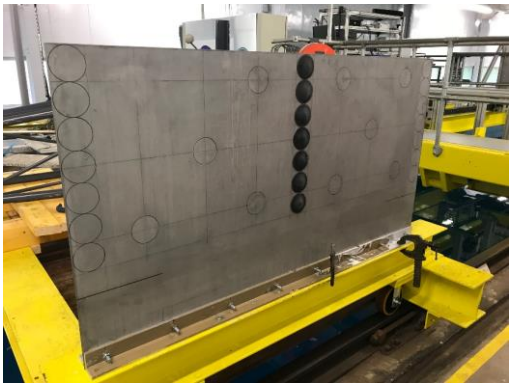

c)  d) 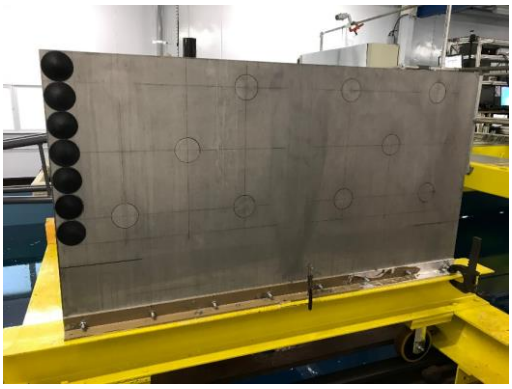

Figure 5 - Tubercles Configurations:
a) Distributed; b) Mid-length; c) Upstream; d) Downstream

The rows of 7 tubercles were positioned at the Upstream edge, at Mid-length, and at the Downstream edge of the plate. The distributed configuration counts 11 tubercles on each side, equally spaced to cover the whole wetted area of the plate. Both sides of the plate were fitted symmetrically with the same number and position of tubercles.

The experimental tests of these configurations were similar to the CFD simulations performed by [33]. The distributed configuration is a simplified representation of the actual upside part of the head of a typical humpback whale calf. It was in the authors' intention to understand how such a surface would have changed the drag of a flat plate.

4. Results

This section presents the results at a nominal temperature of 15°C. The complete data of the tests at the actual temperature of the water (Tm) of 17°C and the extrapolated temperature (T) at 15°C are not reported here.
The relation between the total resistance coefficient (C_T) was given according to Equation (7):

$$C_T(15°) = C_T(Tm) + [C_F(15°) - C_F(Tm)] \quad (6)$$

The total resistance coefficients (C_T) obtained from the experimental tests is plotted against the Reynolds number (Rn) in the *Figure 6* below:

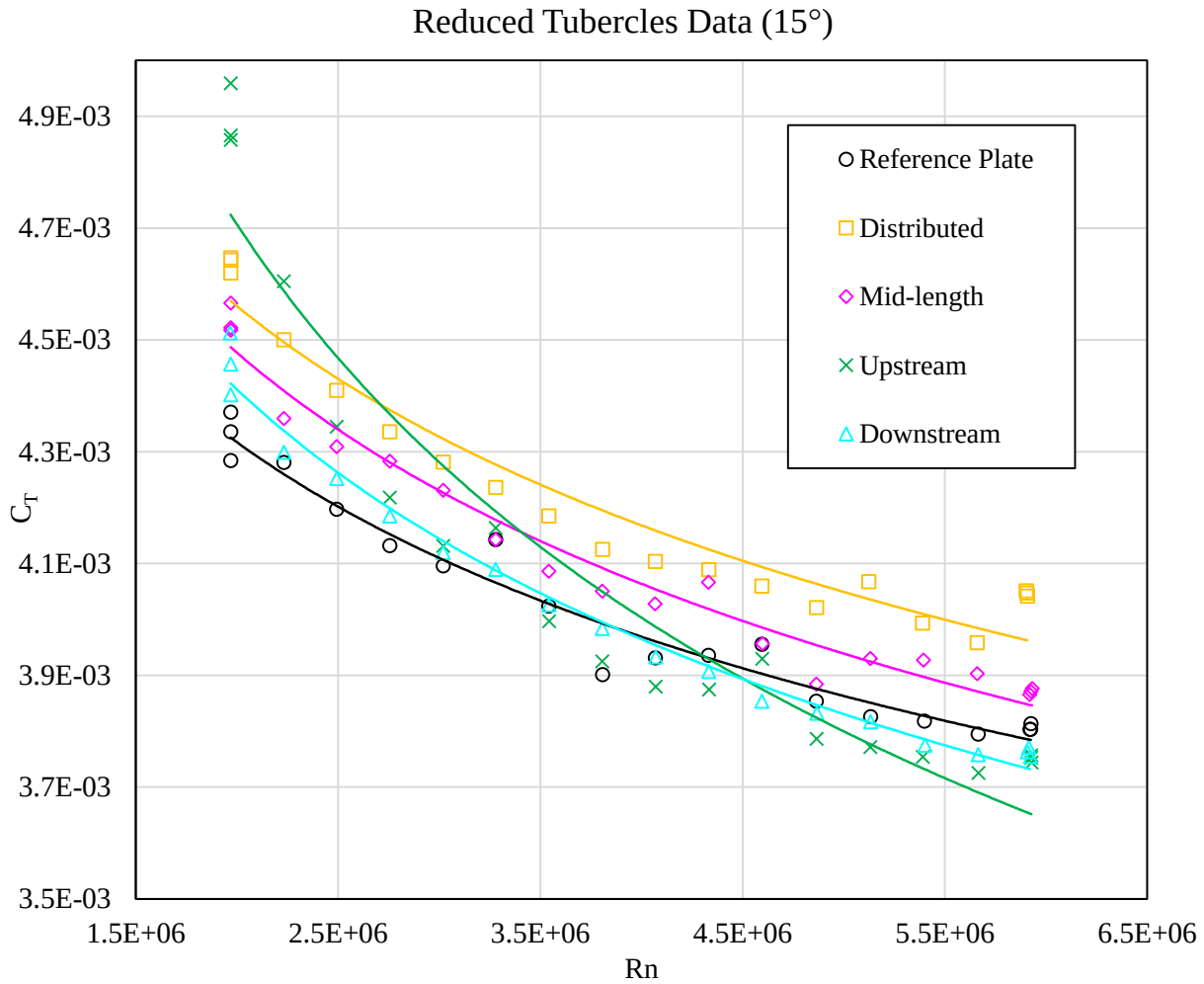

Figure 6 - Experimental results: C_T curves for the whole range of speed tested

As it can be seen, despite the peaks observed at different Reynolds number, all the C_T curves present a decreasing trend. The steeper curve is of the leading-edge configuration while a flatter behaviour characterises the reference plate.

A comparison between the drag and C_T experimental data at 15°C for the smooth reference plate and the tubercles configurations are presented in the *Table 3*.
The values corresponding to the Leading-edge and Trailing-edge configurations which are highlighted in green, represent the beneficial reductions obtained.
The trend of the total resistance coefficient curve of the leading-edge configuration in *Figure 8* is neatly showing the benefits in terms of resistance at high speeds. Indeed, for this configuration, at high speeds, the values of C_T are up to 1.8418% minor than those of the reference plate.
For the Distributed and Mid-length configurations the red values underline the degraded performances.

Table 3 – Experimental Data at 15°C for velocities between 3.7 and 4.5 m/s: variation of drag and C_T with respect to the reference plate

Reference	**V [m/s]**	3.7052	3.9106	4.1131	4.3145	4.5121
	Drag [N]	46.4422	51.3657	56.7144	62.0289	67.9979
	CT (15°)	3.8533E-03	3.8257E-03	3.8180E-03	3.7947E-03	3.8032E-03
	Rn (15°)	4.8632E+06	5.1328E+06	5.3985E+06	5.6630E+06	5.9222E+06
Distributed	**Δ Drag %**	5.9963	7.4787	5.7417	5.7015	7.2535
	Δ CT %	4.3528	6.3233	4.5862	4.3014	6.5131
Mid-length	**Δ Drag %**	2.7453	3.2679	2.7262	2.9473	2.4883
	Δ CT %	2.7692	3.4361	2.9876	3.1242	2.6644
Upstream	**Δ Drag %**	-0.9629	-0.7974	-1.2758	-1.0686	-0.4145
	Δ CT %	-1.7406	-1.4149	-1.6768	-1.8418	-1.2162
Downstream	**Δ Drag %**	0.3109	0.4717	-0.3520	-0.2573	-0.5365
	Δ CT %	-0.5593	-0.2326	-1.1243	-0.9660	-1.0631

For each run, the actual speed of the carriage was taken into account rather than the input one.
As expected, the distributed configuration presents an increase of drag for the whole range of speed. At 4.5 m/s there is an average increment of 6,3026%. On the other hand, one can appreciate the benefits of the leading-edge and trailing-edge configurations in terms of drag and resistance coefficients. At high Reynolds numbers (velocities higher than 3.7 m/s there is a drag reduction also appreciable in the C_T curve. Also, the trailing-edge configurations shows similar results at high Reynolds number. The best result is obtained for the leading-edge configuration at 4.5 m/s, highest speed of the range, with an average drag reduction of -1.4567%. Whereas, at the same speed, for the distributed configuration is registered the greatest penalty of drag is +7.1569%.
Since the values of the side force registered by the transducer were satisfactorily small for the reference plate and only slight ineffective variations occurred for the other configurations tested, the data are not presented here.
Following the procedure of [41] and [43] to carry out an uncertainty analysis as explained in the Methodology section, here are presented the results for the tubercles configurations tested.

Table 4 - Uncertainty Analysis of C_T at the lowest and highest speed of the range

		1.5 m/s			4,5 m/s		
		Bias	**Precision**	**Uncertainty**	**Bias**	**Precision**	**Uncertainty**
Reference	[-]	3.2148E-05	3.36673E-05	4.6551E-05	1.9287E-05	5.35295E-06	2.0016E-05
	[%]	0.7361	0.7706	1.0624	0.5041	0.1404	0.5278
Distributed	[-]	3.3484E-05	1.37817E-05	3.6209E-05	2.0653E-05	4.52922E-06	2.1144E-05
	[%]	0.7170	0.2964	0.7749	0.5078	0.1118	0.5198
Mid-length	[-]	3.2981E-05	2.54072E-05	4.1633E-05	1.9754E-05	5.07195E-06	2.0395E-05
	[%]	0.7220	0.5571	0.9097	0.5077	0.1309	0.5241
Upstream	[-]	3.4268E-05	5.31643E-05	6.3252E-05	1.9163E-05	1.28953E-05	2.3098E-05
	[%]	0.6953	1.0746	1.2759	0.3900	0.2628	0.4697
Downstream	[-]	3.2707E-05	5.22021E-05	6.1602E-05	1.9289E-05	3.03337E-05	3.5947E-05
	[%]	0.7285	1.1577	1.3633	0.5063	0.7939	0.9394

For the Upstream test, the combined bias uncertainty of the devices for C_T ranges between ±0,6953%. As it can be seen from *Table 4*, the overall uncertainty in C_T ranges between ±1,2759% at the lowest speed, and between ±0,4697% at the highest speed. For the frictional resistance coefficient C_F the overall uncertainty results are generally lower than those of the total resistance coefficient but are not reported in this paper.For all the tests, the overall uncertainty levels of the drag coefficients are sufficient when compared to other experiments given in the literature such as [44].

5. Conclusions and Recommendations

The towing tank experiments carried out at Kelvin Hydrodynamics Laboratory for this paper focused on the effect of biomimetic tubercles on the hydrodynamic efficiency of a flat plate. For the tests, a stainless-steel flat plate with main dimensions of 1.5x0.8x0.005 m was rigged on the carriage and towed at a range of speed from 1.5 to 4.5 m/s while the transducers measured its drag and side forces. The configurations of biomimetic tubercles tested were four, namely “Distributed”, “Mid-length row”, “Upstream row” and “Downstream row”. In this case, the main objective was to find the configuration which would have given the best improvement on the performances of the plate. The values of drag measured in the tank were compared and then non-dimensionalised to find the resistance coefficients.To assure the acceptable reliability of the data, an uncertainty analysis of the drag coefficients was conducted for all of the present experiments and compared to other studies given in the literature such as [44].

The findings of the experimental investigation carried out in this paper gave promising results for a practical application of 3-D printed biomimetic tubercles to reduce the hydrodynamic resistance of a flat plate. The quantitative data collected suggested that the most prominent effects is a drag reduction at higher Reynolds number, especially for the Upstream and Downstream configurations of the rows of tubercles. For these setups, the towing tank tests revealed an appreciable lower resistance with respect to the bare flat plate of -1.3% and -0,5%, respectively. The trend of the total resistance coefficients suggested that at higher Reynolds number those reductions would grow.

On the other hand, the opposite findings were made for the Distributed and Mid-length configurations where a maximum increase of 7.5% and 3.3% were registered. The application of such distributed and mid-length arrangements, despite the slight drag increase, could be justified to obtain a conveniently manipulated flow over the plate.

Despite the uncertainty in the flow mechanisms responsible of the tubercle effect, an array of theories claimed that the addition of tubercles increases the hydrodynamic performance. A future EFD study might be to test other types of tubercles configurations and obtain roughness function models to

employ in a CFD software code in order to predict the full-scale effect on ships. Very limited is the research into the effects of tubercles on the component of drag of marine structures, either a simple flat plate or a ship hull. In that perspective, not only different shapes and dimensions, but also different positions of the biomimetic tubercles on the plate can be studied. Indeed, the models described in this paper can be easily variegated and eventually upgraded to more sophisticated arrangements.

6. References

[1] J. F. V. Vincent, O. A. Bogatyreva, N. R. Bogatyrev, A. Bowyer, and A.-K. Pahl, "Biomimetics: its practice and theory," *J. R. Soc. Interface*, vol. 3, no. 9, p. 471, 2006.

[2] J. M. Benyus, *Biomimicry : innovation inspired by nature*. Morrow, 1997.

[3] S. Vogel, *Cats' paws and catapults : mechanical worlds of nature and people*. Norton, 1998.

[4] P. Forbes, *The gecko's foot : bio-inspiration : engineering new materials from nature*. New York: W.W. Norton & Co, 2006.

[5] Y. Bar-Cohen, "Biomimetics—using nature to inspire human innovation," *Bioinspir. Biomim.*, vol. 1, no. 1, pp. P1–P12, Mar. 2006.

[6] Mueller Tom, "Biomimetics: Design by nature," *Natl. Geogr. Mag.*, 2006.

[7] R. Allen, "Bulletproof feathers: how science uses nature's secrets to design cutting-edge technology," *Choice Rev. Online*, vol. 48, no. 05, pp. 48-2633-48–2633, 2013.

[8] F. E. Fish, P. W. Weber, M. M. Murray, and L. E. Howle, "The tubercles on humpback whales' flippers: Application of bio-inspired technology," *Integr. Comp. Biol.*, vol. 51, no. 1, pp. 203–213, 2011.

[9] G. Taubes, "Biologists and engineers create a new generation of robots that imitate life," *science.sciencemag.org*, 2000.

[10] F. E. Fish, "Limits of nature and advances of technology: What does biomimetics have to offer to aquatic robots?," *Appl. Bionics Biomech.*, vol. 3, no. 1, pp. 49–60, Jan. 2006.

[11] F. E. Fish, "Biomimetics: determining engineering opportunities from nature," 2009, vol. 7401, p. 740109.

[12] K. Mohseni, R. Mittal, and FE Fish - Bioinspiration & Biomimetics, "Special issue featuring selected papers from the Mini-Symposium on Biomimetic & Bio-Inspired Propulsion (Boulder, CO, USA, 26 June 2006)," *Bioinspir. Biomim.*, 2006.

[13] IMO, "Third IMO GHG Study 2014 Executive Summary and Final Report," 2015.

[14] Y. K. Demirel, "Modelling the Roughness Effects of Marine Coatings and Biofouling on Ship Frictional Resistance," 2015.

[15] IMO, "Inclusion of regulations on energy efficiency for ships in MARPOL Annex VI," 2011.

[16] J. D. van Manen and P. van Oossanen, *Principles of Naval Architecture*, Second Rev., vol. II. The Society of Naval Architects and Marine Engineers, 1988.

[17] H. Lackenby, "The Thirty-Fourth Thomas Lowe Gray Lecture: Resistance of Ships, with Special Reference to Skin Friction and Hull Surface Condition," *Proc. Inst. Mech. Eng.*, vol. 176, no. 1, pp. 981–1014, Jun. 1962.

[18] ITTC, "Final Report and Recommendations to the 28th ITTC," 2017.

[19] P. J. Clapham, "Humpback Whale: Megaptera novaeangliae," *Encycl. Mar. Mamm.*, pp. 489–492, Jan. 2018.

[20] P. J. Clapham and J. G. Mead, "Megaptera novaeangliae," vol. 3, no. 604, pp. 1–9, 1999.

[21] E. Mercado, "Short Note: Tubercles: What Sense Is There?," *Aquat. Mamm.*, vol. 40, no. 1, pp. 95–103, Mar. 2014.

[22] F. E. Fish and G. V. Lauder, "Passive and Active Flow Control by Swimming Fishes and Mammals," *Annu. Rev. Fluid Mech.*, vol. 38, no. 1, pp. 193–224, Jan. 2006.

[23] W. Shi, M. Atlar, R. Norman, B. Aktas, and S. Turkmen, "Numerical optimization and experimental validation for a tidal turbine blade with leading-edge tubercles," *Renew.*

Energy, vol. 96, pp. 42–55., 2016.
[24] W. Shi, M. Atlar, R. Norman, B. Aktas, and S. Turkmen, “Biomimetic improvement for a tidal turbine blade,” 2015.
[25] S. M. Hasheminejad, H. Mitsudharmadi, S. H. Winoto, and S. H. Winoto, “Effect of Flat Plate Leading Edge Pattern on Structure of Streamwise Vortices Generated in Its Boundary Layer,” *Artic. J. Flow Control*, vol. 2, pp. 18–23, 2013.
[26] D. S. Miklosovic, M. M. Murray, L. E. Howle, and F. E. Fish, “Leading-edge tubercles delay stall on humpback whale "Megaptera novaeangliae… flippers,” *Phys. FLUIDS*, vol. 16, no. 5, 2004.
[27] M. D. Bolzon, R. M. Kelso, and M. Arjomandi, “Tubercles and Their Applications,” *J. Aerosp. Eng.*, vol. 29, no. 1, p. 04015013, Jan. 2016.
[28] A. Dobre, H. Hangan, and B. J. Vickery, “Wake Control Based on Spanwise Sinusoidal Perturbations,” *AIAA J.*, vol. 44, no. 3, pp. 485–492, Mar. 2006.
[29] P. W. Weber, L. E. Howle, M. M. Murray, and F. E. Fish, “Lift and drag performance of odontocete cetacean flippers,” *J. Exp. Biol.*, vol. 212, no. 14, pp. 2149–2158, Jul. 2009.
[30] W. Shi, M. Atlar, R. Rosli, B. Aktas, and R. Norman, “Cavitation observations and noise measurements of horizontal axis tidal turbines with biomimetic blade leading-edge designs,” *Ocean Eng.*, vol. 121, pp. 143–155, Jul. 2016.
[31] T. Gruber, M. M. Murray, and D. W. Fredriksson, “Effect of Humpback Whale Inspired Tubercles on Marine Tidal Turbine Blades,” in *Volume 2: Biomedical and Biotechnology Engineering; Nanoengineering for Medicine and Biology*, 2011, pp. 851–857.
[32] W. Shi, M. Atlar, and R. Norman, “Detailed flow measurement of the field around tidal turbines with and without biomimetic leading-edge tubercles,” *Renew. Energy*, vol. 111, pp. 688–707, Oct. 2017.
[33] A. Marino, M. Atlar, and Y. K. Demirel, “An investigation of the effect of biomimetic tubercles on a flat plate,” in *ASME 2019 38th International Conference on Ocean, Offshore and Arctic Engineering, OMAE 2019*, 2019.
[34] M. P. Schultz, “Effects of coating roughness and biofouling on ship resistance and powering,” *Biofouling*, vol. 23, no. 5, pp. 331–341, Oct. 2007.
[35] Y. K. Demirel, “Personal Communication.” Glasgow, 2019.
[36] ITTC, “ITTC-Recommended Procedures and Guidelines,” 2011.
[37] M. P. Schultz and K. A. Flack, “The rough-wall turbulent boundary layer from the hydraulically smooth to the fully rough regime,” *J. Fluid Mech.*, vol. 580, pp. 381–405, Jun. 2007.
[38] G. Hughes, “Frictional resistance of smooth plane surfaces in turbulent flow,” *Trans. Ina*, vol. 94, 1952.
[39] G. Hughes, “Friction and form resistance in turbulent flow and a proposed formulation for use in model and ship correlation,” *Trans. Ina*, vol. 96, 1954.
[40] “Kelvin Hydrodynamics Laboratory | University of Strathclyde.” [Online]. Available: https://www.strath.ac.uk/engineering/navalarchitectureoceanmarineengineering/ourfacilities/kelvinhydrodynamicslaboratory/.
[41] ITTC, “ITTC Uncertainty Analysis, Example for Resistance Test. ITTC Recommended Procedures and Guidelines, Procedure 7.5-02-02-02, Revision 01.,” 2002.
[42] ITTC, “ITTC-Recommended Procedures and Guidelines Uncertainty Analysis, Instrument Cali-bration ITTC Quality System Manual Recommended Procedures and Guidelines Procedure,” 2017.
[43] H. W. Coleman and W. G. Steele, *Experimentation, validation, and uncertainty analysis for engineers*. 1999.
[44] M. P. Schultz, “The Relationship Between Frictional Resistance and Roughness for Surfaces Smoothed by Sanding,” *J. Fluids Eng.*, vol. 124, no. 2, p. 492, Jun. 2002.